A Smart Servo Feed Drive for Electro Discharge Machining Systems Industrial Applications Using Piezoelectric Technology

M. Shafik[1] & H. S. Abdalla[2]

[1]School of Technology, Faculty of Art & Design and Technology, University of Derby, Derby, UK

[2]School of Architecture, Computing and Engineering, University of East London, London, UK

m.shafik@derby.ac.uk

Abstract

This paper presented a smart servo control feed-drive for electro discharge systems machining and processing industrial applications. The servo control drive consists of three main components, a linear piezoelectric ultrasonic motor, piezoelectric ultrasonic drive and servo control unit. On this paper, the linear ultrasonic analysis, design and development process has been discussed. The test and validation of the servo control feed drive in Electro Discharge machining and processing system industrial applications has also been presented. The linear piezoelectric ultrasonic motor consists of three parts, the stator, rotor and sliding element. The linear ultrasonic motor development life cycle, design and structure, mechanism of motion, Finite Element analysis, and experimental examination of the characteristics has been discussed in this paper. The electronic driver of the ultrasonic motor consists of two main stages which are the booster and piezoelectric amplifier. The piezo amplifier designed of four output transistors, a push-pull and bridge, were connected in order to achieve the necessary electrical parameters, to drive and control the servo feed drive travelling speed. The inter-electrode voltage, current and radio frequency signal has been used to control the system machining process. The essential experimental arrangement to implement and examine the developed servo feed drive in Electro Discharge system was carried out. The initial results showed that the servo drive was able to provide a bidirectional of motion, no-load travelling speed equal to 28 mm per second, maximum load of 1.8 Newton, a resolution less than 50μm and a dynamic time response less than 10 msec. The electron microscopic micro examination into the processed samples indicated that the new ultrasonic servo drive showed a clear improvement in the surface profile of the machined materials, system stability, a notable reduction in the processing time, arcing and short-circuiting teething phenomena. This was verified by assessing the electrode movements, the variations of the inter-electrode gap voltage, current and feedback control signals.

Keywords

Ultrasonic Drive; Micro Actuators; EDM; EDT; Mechatronics

Introduction

Servo control feed drives using DC and or AC servomotors have been known for more than a hundred of years and have many applications in the areas of manfacuring process and machine control. Machining and process control can be classified according to the level of precision and dynamic response as normal machining, precision, high precision and ultra-high precision machining. It is understood that higher accuracy, finer resolution and fast dynamic response are essential for high precision machining and manufacturing processes. In the mid 1940s, servo control feed drives using DC/AC servomotor technology were implemented in Electro Discharge Machining (EDM) applications. EDM applications are classified as high precision machining. The main principle of operation of EDM is based mainly on a spark discharge between two conducting surfaces separated by a dielectric medium. The generated spark duration is on the order of microseconds and the inter-electrode gap size is of 10 to 100 micrometers. EDM is widely used in various applications including machining different complex and intricate shapes, slots, drilling holes, cutting and texturing. The actual texturing process well-known as Electro Discharge Texturing (EDT) generally has a multi rotary motor/ballscrew/slide/slideway arrangement in a small volume [Shafik, M., 2003, Shafik M. & H. S. Abdalla, 2011, Shafik M., Knight J. and Abdalla H. 2001, Simao J, Aspinwall D, El-Menshawy F and Ken Meadows K., 2002]. The function is to focus as many electrodes on a given area as possible, given the limitations of the design constraints that is dominated by the physical size and volume of DC and or AC servomotors and the other kinematic elements required to effect rotary to linear motion. Texturing is a process of creating irregularities, with regular or irregular spacing that

tends to form patterns or texture on the surface. Texture contains roughness and waviness that can assist in providing the inherent quality of any subsequent paint finish, appearance and lifetime. Since the requirements of high precision and accurate machining of EDT applications never stop rising, much of the research has been concerned with the servo control feed drive level of precision, stability, dynamic response and surface profile of the processed products. Some authors have identified these problems [Behrens, A., and Ginzel, J., 2001, Behrens, A., Ginzel, J. and Bruhns, F., 2001]. Success in presenting a realistic solution to these problems has been limited. Thus there is a need to develop a new servo control feed drive using innovative technology that could provide high precision, fast dynamic response and robust stability.

Piezoelectric ultrasonic motor (USM) technology offers many opportunities in the field of high precision servo positioning control [Lin, F. J., Wai R. J. and Hong C. M., 2000, Izuno, Y., Izumi, T., Yasutsune, H., Hiraki, E. and Nakaoka, M., 1998]. It has been used widely in both instrumentation and machine tool applications such as, EDM [Shafik M. & H. S. Abdalla, 2011], EDT [Shafik M., Knight J. and Abdalla H. 2001], micro-machining [Shafik, M., 2003, Shafik M. & H. S. Abdalla, 2011, Shafik M., Knight J. and Abdalla H. 2001], artificial prostheses [Ise, et al, 1991], auto focusing drives for single-lens reflex cameras [Hosoe, 1989], rotary supports for video cameras and artificial heart actuators. These applications show that piezoelectric USM servo control systems can be more effective than DC and or AC servomotor drives whenever high and ultrahigh precision level of control is required. This is due to their high resolution, high stiffness, large output force, compactness and quick dynamic response despite their limited positioning ranges. These distinctive features presented a challenge to design a new servo control feed drive using piezoelectric USMs technology to improve EDT servo control system degree of precision, dynamic response, performance and extend its capabilities to include more accurate machining.

The potential advantages of the developed servo control feed drive using piezoelectric ultrasonic technology are its direct drive, fine position, high resolution, dynamic time response and compact size in comparison to a DC and or AC servomotors, thus allowing the possibility of bringing to fruition a design for an EDT servo head that has the ability to effect many electrodes, each separately servo controllable, on a given area. The piezoelectric Linear Ultrasonic Motor (USM) drive has the same kinematics capability as a rotary motor/ballscrew/slide/slideway arrangement and is controllable within the limits that DC/AC servos operate.

The piezoelectric ultrasonic servo drive structure principally depends on the industrial application design specifications [Shafik, M., 2003, Shafik M. & H. S. Abdalla, 2011, Shafik M., Knight J. and Abdalla H. 2001, Furutani, K. and Furuta, A. March,, 2008, Zhang , F., Chen, W., Lin, J. and Wang, Z., 2005, Chen, Y., Lu, K., Zhou, T.Y., Liu, T. and Lu, C.Y., 2006, Li, X., Chen, W.S., Tang, X. and Liu, J.K., 2007, Frangi, A., Corigliano, A., Binci, M. and Faure, P., 2005, Aoyagi M., Tomikawa Y. and Takano T., 1992, Aoyagi M. and Tomikawa Y., 1996, Chiharu K, et al., 1998, M. Shafik, et al, 2012, Shafik M., et al, 2012, Ming, Y. and Que, P. W., 2001]. Potentially, they offer a significant flexibility for position and feed-rate control [Lebrun, L., et al., 1999, Takano T., Tomikawa Y. and Takano C.K., 1999, He S., Chen W., Tao X., and Chen Z., 1998, Newton D., Garcia E. and Horner G. C., 1997]. They have compact size, high force density, simple mechanical construction, low weight, slow speed without additional gear or spindle, high torque, non-magnetic operation, freedom for constructional design, very low inertia, fast dynamic time responses, direct drive, fine position resolution, miniaturization and noiseless operation. These criteria give them the potential to replace electromagnetic motors arrangements in a number of industrial applications [Shafik M. & H. S. Abdalla, 2011, Shafik M., Knight J. and Abdalla H. 2001].

Demanding and careful examination for these applications reveals that there are apparent shortcomings. The first shortcoming is in regard to the dynamic time response of the motor and its transfer function. While a piezo-ceramic element (typically Lead zirconate titanate (PZT)) expands in direct proportion to the magnitude of the applied voltage, the USM on the other hand accumulates those displacements over time. Therefore the transfer function of the USM, related to the magnitude of the driving signal to the displacement is an integrator [Zhang B. and Zhenqi Z., 1997, Tal, J. 1999] and this shows a delay in the dynamic response of the USM, but it is not nearly significant as that in an electromagnetic servomotor. The second shortcoming is that because motion is transmitted through a friction force, it will have a dead band due to the friction. Often USM does not move until the input signal is

greater than 10% of the maximum allowed voltage to overcome the friction. Such a dead band limits the ability of a USM to accelerate quickly and position accurately [Shafik M. & H. S. Abdalla, 2011, Shafik M., Knight J. and Abdalla H. 2001, Tal, J. 1999].

Overall Design, Analysis and Development of the USM

The overall design of the developed USM has taken into consideration application needs such as type of motion, degree of resolution, travelling speed, output force required, load capacity, torque, compactness, integration of the parts into the frame of the motor, production of the parts, maintenance and sustainability. The design process of the linear USM have passed through a number of phases, the first of which focused on the motor arrangement that meets the EDM/EDT application requirements, second one focsed on the structure and final one in the principles of motion.

Structure of the Proposed Linear Piezoelectric USM

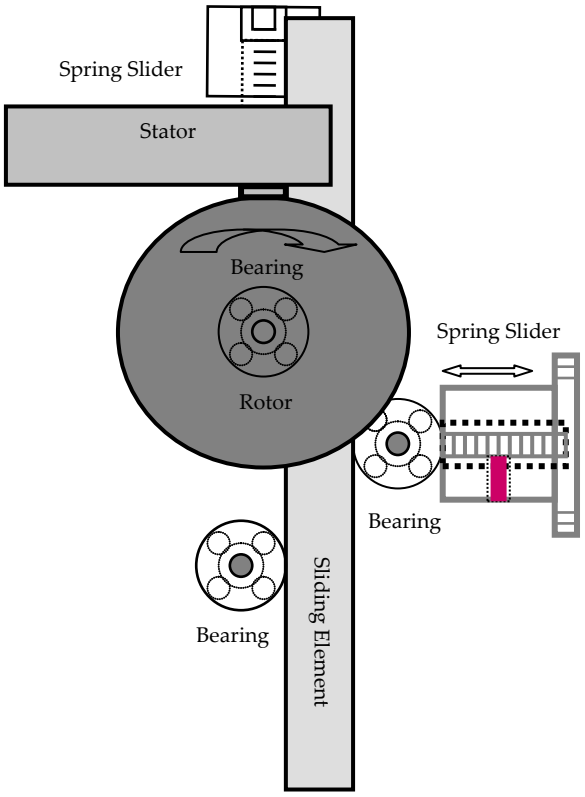

FIG. 1 PROPOSED DUAL MODE STANDING WAVE LINEAR USM USING A SINGLE FLEXURAL VIBRATION TRANSDUCER FOR EDT INDUSTRIAL APPLICATIONS [SHAFIK, M., 2003]

Fig. 1 shows the motor structureand consists of three main parts which are the stator, rotor and sliding element. The stator is a single flexural vibrating transducer made from Lead Ziconate Titanate (PZT) piezoceramics material. The rotor is composed of the motor driving wheel and the shaft. The sliding element is made up of rectangular tube steel. The stator, rotor and sliding element jointly with the frame of the motor form the linear structure of the USM.

The principles of working is based on creating elliptical micro motions of surface points generated by superposition of longitudinal and bending vibration modes of oscillating structures [Aoyagi M. and Tomikawa Y., 1996, Chiharu K, et al., 19987]. By pressing the rotor against the driving tip of the stator, the micro motions are converted into a rotary and linear motion, through the friction between parts of the motor. However, to create a strong second bending vibration mode, the polarisation direction of the piezoelectric vibrator perpendicular to the electrodes, the piezoelectric ceramic vibrator was arranged as shown in Fig. 2.

The longitudinal and bending vibration modes are coupled by asymmetry of the piezoelectric ceramic vibrator [Aoyagi M., Tomikawa Y. and Takano T., 1992, Tobias H. and Wallaschek J., 2000, Snitka V., 2000]. The first surface of the piezoelectric transducer is segmented into four sub-surfaces which are arranged electrically to provide two sub-electrodes, named A and B. The second surface is connected to the earth and named electrode C. Then a single-phase AC signal with a wide frequency band is used to obtain the electrode natural operating frequency. Driving the electrode A and C by a single phase AC signal with a frequency closer to the resonant frequency of the vibrator provides one direction of motion and switching to electrode B, and changes the bending vibration mode by a phase shift of 180 degrees, which leads to reversing the direction of motions as shown in Fig. 3. Few authors have used these phenomena and succeeded to develop different structures to generate linear motion [Aoyagi M., 1992, Aoyagi M. and Tomikawa Y., 1996, Snitka V., 2000, www.nanomotion.net].

Snitka V., 2000 and Aoyagi M., 1992 showed that the load of this type of motor depended on the contact point of the rotor, the dimension of the piezoelectric elements and material of the stator and the rotor. Snitka V.,2000 proved that the pre-load pressing forces and friction between parts influenced the degree of accuracy obtainable. Therefore, the material for the moving parts of the proposed motor has been carefully selected.

It was also noticed that the slide element did not move until the excitation voltage reaches about half wave its maximum value, because a single driving system with constant frequency has been used to create both normal and thrust force, which reduced the fine micro resolution of the USM. The thrust force must overcome the static friction force between the motor parts, result of pre-load force, to allow relative motion between the stator and the rotor [Takano T., Tomikawa Y. and Takano C.K., 1999]. In the developed design, a coil spring was used to press the vibrating transducer against the rotor and enabled the pre-load force to be sensitively adjusted.

Working Principles of the Proposed USM

The USM motor was designed using standing wave vibrations with a fixed wave length. The perception is to utilise two oscillation modes of vibration to obtain desired motion of the piezoelectric vibrating transducer longitudinal and transverse vibration modes, of which one vibration produces a normal force, while the other vibration generates thrust force, which is perpendicular to the normal force, resulting in a micro elliptical trajectory of motion, at the vibration transducer tip, by attaching the stator tip to the rotor using a coil spring. The micro elliptical trajectory is converted into a rotary motion, as shown in Fig. 3 As the combination of two modes of vibrations created a friction based driving force between the stator and the rotor at the contact tip, a movement in forward or backward direction was created depending on the methodology used to electrify the piezoelectric ceramic transducer to generate two modes of vibrations.

The linear motion was developed using the friction based driving force between the shaft and the sliding element of the motor as shown in Fig. 1.

Modelling and Analysis Using Finite Element of the Proposed USM

Piezoelectric USM's have many complex non-linear characteristics and modelling them is an essential step of the design and development lifecycle. There are two methods of modelling and analysis can be used to simulate and model piezoelectric USM's [Shafik M., Knight J., 2002, Lin M. W., Abatan A. O. and Rogers C. A., 1994, Hwang W. S. and Park H. C., 1993]. These methods are the analytical analysis and finite element analysis (FEA) method. In the current developed USM development process, ANSYS FEA software was used to examine the proposed motor structure, investigate the material vibration modes, identify the transducer material, and obtain the technical operating parameters. It also helped to optimise the motor performance through investigating the variation of the displacement versus the frequency.

Two types of FEA were used, model analysis and harmonic analysis. These offer two types of loads, the nodal and the pertaining to the element. In the nodal case, the loads were applied to nodes of the element that do not have direct links with element properties.

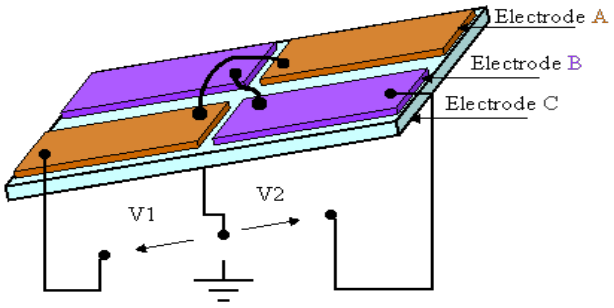

FIG. 2 USM STATOR CONNECTIONS ARRANGEMENTS AND PRINCIPLES USED TO GENERATE TWO DIRECTIONS OF MOTION [SHAFIK, M., 2003]

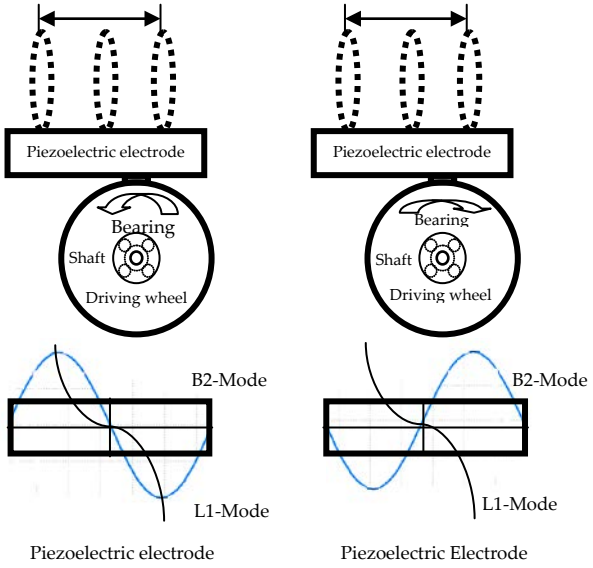

FIG. 3 PRACTICE USED TO CREATE BIDIRECTIONAL OF MOTION USING TRANSVERSE BENDING VIBRATION MODES AT A FREQUENCY CLOSE TO LONGITUDINAL VIBRATION MODE [SHAFIK, M., 2003]

The USM model was built based on a full consideration of the motor boundary conditions and EDT industrial application requirements. The stator was defined as the active element and the rotor was defined as the passive element. Fig 4 (a) and (b) show the variation of displacement of the stator versus the frequency, for rotary and linear structure, of the motor. It illustrates the change of displacement versus the frequencyand also shows the resonant frequency of

the current model-42.2 kHz. This is helped to determine the vibration amplitude, thrust force and optimise motor structure performance.

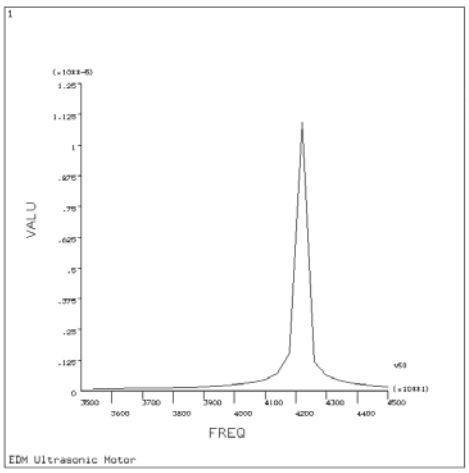

(a)

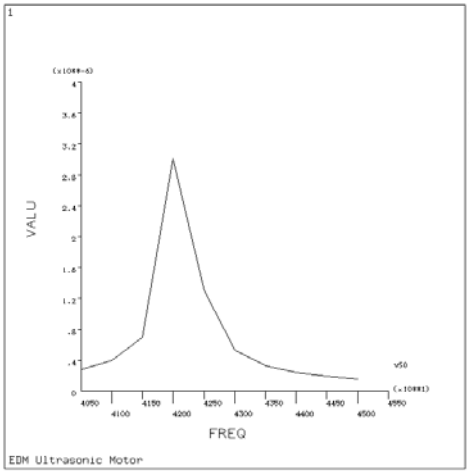

(b)

FIG. 4 THE STATOR (VIBRATION TRANSDUCER) DISPLACEMENT VERSUS THE FREQUENCY FOR THE DEVELOPED LINEAR USM (AC 50V) (A) FOR ROTARY STRUCTURE (B) FOR LINEAR STRUCTURE [SHAFIK, M., 2003]

The USM motor linear arrangement model analysis has shown that there are some impacts of the sliding element on the transducer deformation modes of vibration and the possible maximum displacement. The displacement of the transducer changed from 10.1125 μm to 3.0999 μm. The analysis also enabled the assessment on the motor possible generated amplitude of vibration, thrust force, material modes of vibration and the distribution of the vibration wave of the transducer, which helped to avoid design errors and mishandling of the material deformation.

Material deformation can produce a jerking effect that affects the resolution and degree of accuracy of the motor. Consequently, it could restrict the potential applications of the USM motor and the servo drive fine position as a whole. The motor model-vibration modes for different input signal were determined. Figures 5 and 6 show the two modes of vibration for the motor, the transverse bending mode and longitudinal mode, at the drawn operating frequency.

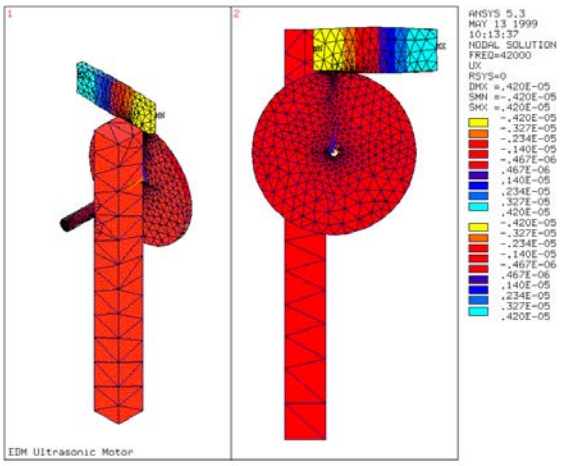

FIG. 5 USM LINEAR STRUCTURE MODEL TRANSVERSE VIBRATION MODE

(FREQUENCY 42200HZ AND AC 50V) [SHAFIK, M., 2003]

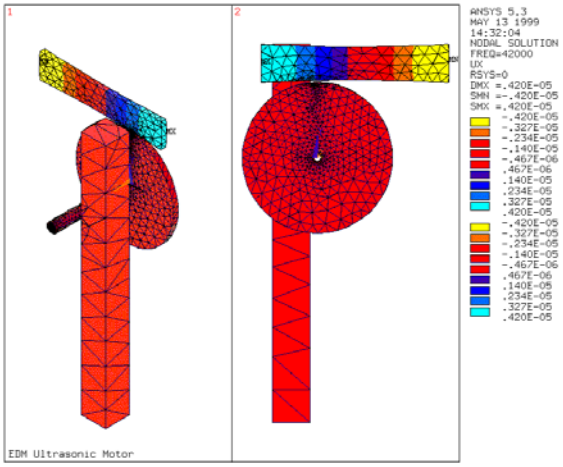

FIG. 6 USM LINEAR STRUCTURE MODEL LONGITUDINAL VIBRATION MODE

(FREQUENCY 42200HZ AND AC 50V) [SHAFIK, M., 2003]

Design of the USM Components

The dimensions of stator for the USM were based on the ratio of frequency of the longitudinal mode f_L and bending mode f_B, $f_L / f_B = 2.0$, and $d / l = 0.1$, as the internal nonlinear coupling of parametric vibration between two resonance modes was generated under these conditions [Behrens, A., Ginzel, J. and Bruhns, F., 2001].

The capacitance ratio and direction of vibratory displacement was also considered. Using the USM models shown in Figures 7 (a) and 7 (b), the relation

between the torque T and various acting forces on the rotor components gives the following relationship:

$$T = F_R \frac{D}{2} = F_r \frac{d}{2} \quad (1)$$

Where, F_R is the micro elliptical force produced using vibration transducer, F_r is the driving force transferred to the shaft using the following torque factor relationship $A_r = D/d$. Where, D is the diameter of the driving wheel and d is the diameter of the shaft.

The torque factor of the USM and the diameter of the rotor (driving wheel and the shaft) were obtained. The transferred force to the shaft was determined using the following torque factor relationship:

$$F_r = F_R \frac{D}{d} \quad (2)$$

This relationship shows that the torque factor A_r has to be carefully considered during the design process of the USM since it influences the efficiency of the driving force produced by the vibration transducer, the resolution of the motor and maximum travelling speed.

The length of the shaft l_s was determined according to the allowable ratio of the l_s/d_s, where d_s is the diameter of the shaft. This is to meet the conceptual view of the design for the proposed motor construction considered the properties of the material used to produce the shaft and the moment of inertia of the rotor that was considered to be small for fast dynamic time response and to obtain a maximum efficiency of the transferred driving force. The pre-load force acting in the shaft and locations of bearings of the sliding element was determined using the dynamic model shown in Fig. 7 (c).

$$\sum F_x = 0.0$$

$$F_{sb} = F_{sh} + F_b \quad (3)$$

Where: F_{sb}, F_b, F_{sh} are the side spring slider, bearing and shaft acting forces, respectively

From the model shown in Fig. 7-c, the bearing acting force F_b was obtained from the following relationship:

$$F_{sb} X = F_b l_{sl} \quad (4)$$

Consequently, the bearing acting force was found to be:

$$F_b = F_{sb} \frac{X}{l_{sl}} \quad (5)$$

Substituting F_b into slider acting force:

$$F_{sb} = F_{sb} \frac{X}{l_{sl}} + F_{sh} \quad (6)$$

Then the shaft acting force was determined using the relationship (7):

$$F_{sh} = F_{sb}(1 - \frac{X}{l_{sl}}) \quad (7)$$

In the proposed design, the side spring slider was located in the middle between the shaft and opposite side bearing, to keep the acting force on the shaft, as minimum as possible (see Fig. 7 (c). The acting force on the shaft in this case was found to be half the slider pre-load acting force.

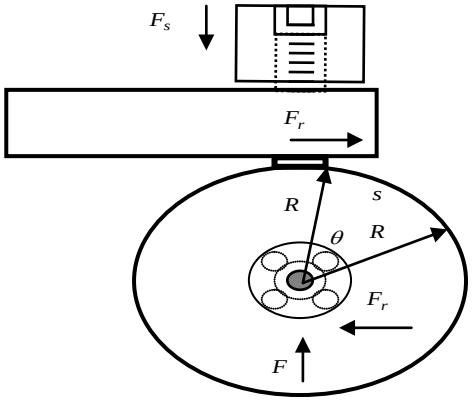

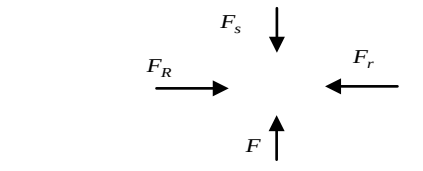

(a)

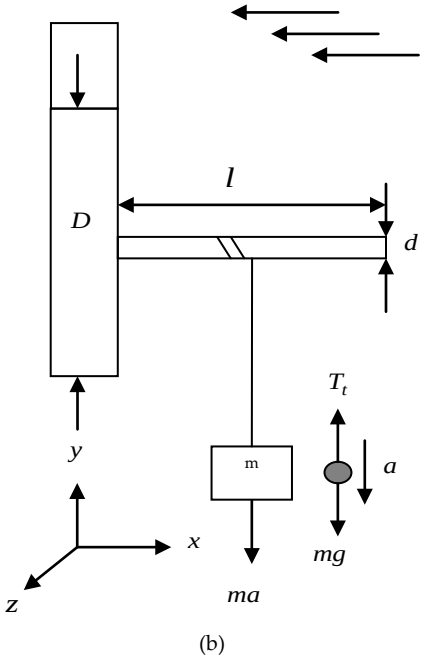

(b)

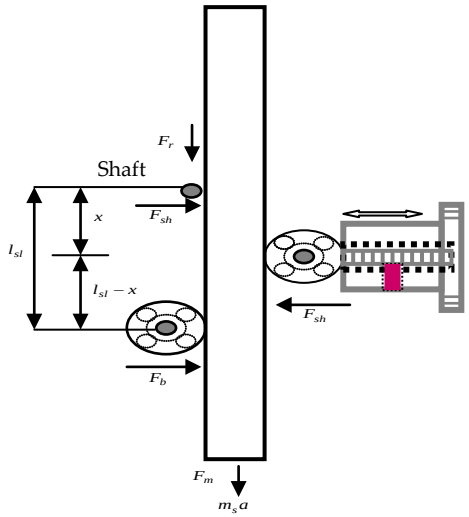

(c)

FIG. 7 DYNAMIC USM MODELS USED TO DETERMINE THE DIMENSIONS OF THE USM PARTS AND OPTIMISE THE BEARING PRELOAD FORCE ON THE USM LINEAR STRUCTURE

Four pins and an interchangeable coil spring were used to house the vibration transducer as shown in Fig. 7 (a). The four pins were used to prevent interference transducer modes of vibrations.

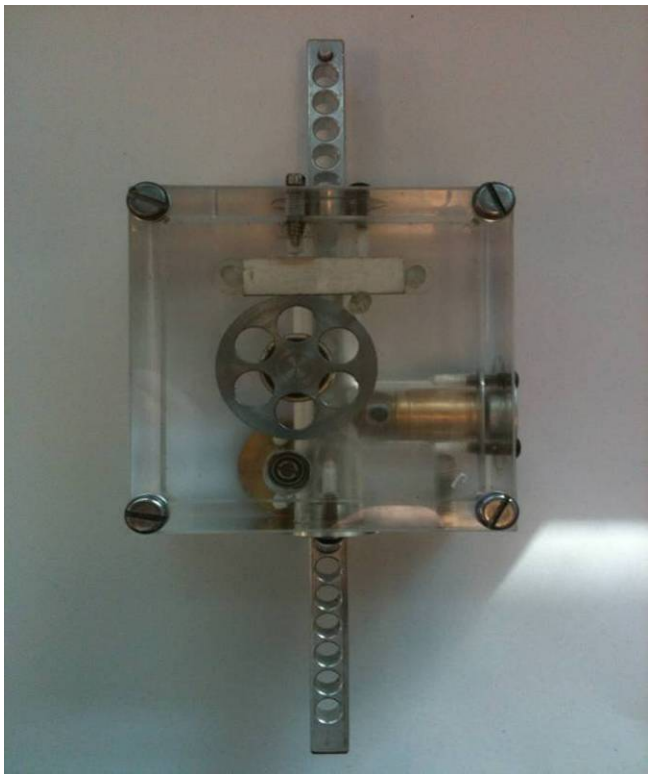

FIG. 8 DEVELOPED ULTRASONIC MOTOR ACTUAL COMPONENTS USING A SINGLE PIEZO-CERAMIC FLEXURAL VIBRATION TRANSDUCER AND FABRICATED PROTOTYPE

The spring was used to support the vibration transducer at the vibration tip as well to keep the stator and rotor in contact. This enabled the vibration transducer to transfer the micro elliptical force into rotational and linear motion using the friction between the USM parts. The optimum pre-load acting force was determined by observing the USM travelling speed versus various forces at the identified operating parameters i.e. voltage, current and frequency. It was clearly noticed that mishandling of the pre-load acting force influenced the motor resolution, stiffness and torque. Two guide-way were also designed and fixed to the top and bottom of the USM frame in order to prevent the sliding element plane motion. Plane motion would affect the accuracy of the USM. The frame of the motor, part of the concept, was designed with a reliable layout to ensure compactness of the design, easy to integrate and maintain the parts of the USM. Fig 8 illustrates the various components of the USM and manufactured prototype.

Experimental Testing of the Developed USM

The main parts of the developed prototype were integrated into the frame of the USM and series of experimental tests carried out. This was aimed to examine the characteristics of the fabricated prototype and EDT industrial application requirements. Initial integration showed that there were some teething problems including irregular rotational and linear motion, resulting from the inaccuracies in the manufacture of the parts of the USM. The irregular rotational speed was due to deviations on the roundness of the driving wheel and irregular travelling speed was from deviations in roundness of the shaft. The roundness of the driving wheel and the shaft were re-machined and retested. The concentricity of the produced parts, such as the rotor, was also tested and showed no error. The parts were reintegrated into the frame of the USM and a series of experimental test was conducted to measure the characteristics of the USM. Fig 9 shows the block diagram of the test rig and Fig. 10 shows the actual system used to examine the prototype. An off-shelf piezoelectric driver was used to supply the vibrating transducer with the AC voltage. Various shapes of AC signal included sinusoidal, saw-tooth and square wave. A display unit, composed of a digital oscilloscope and PC computer, was deployed to trace the signal and determine the USM operating parameters. The travelling speed of the USM was measured via a speedometer. An electro microscope was used to measure the fine resolution of the USM. A programmable switching unit interfaced with a PC computer was applied to control the USM directions of motion and to analyse the measured characteristics.

The operating parameters were measured using the

same USM stator arrangement shown in Fig. 2. The electrodes A and B were connected to a single phase AC power source with a wide range of amplitude and frequency. A switching unit was used to regulate the AC input power for A, B and C electrodes. Fig. 11 shows the relationship between current and voltage of the USM prototype. This help to identify the nature of the USM loadas well to define the USM operating voltage and current. This was found to be voltage: 50 to 100 volts and current: 50 to 100 milliamperes. Then the travelling speed versus the amplitude and frequency of the AC input signal measured, was achieved as follows: the system was connected as shown in Fig. 9 and 10. The frequency of USM driver was altered incrementally.

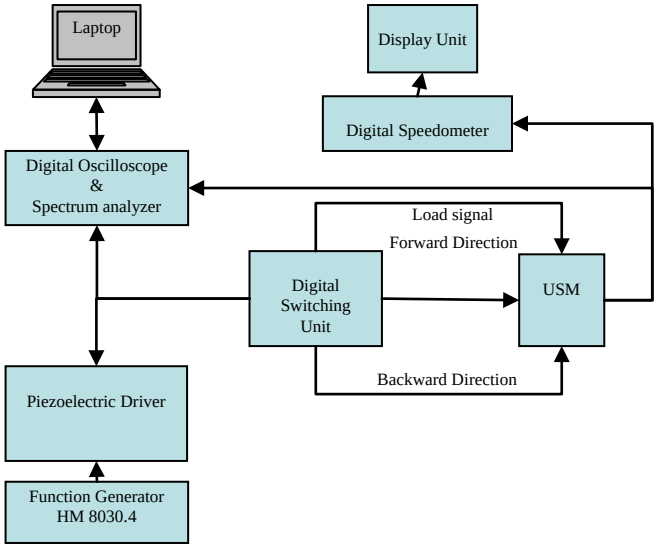

FIG. 9 BLOCK DIAGRAM OF THE TEST RIG ARRANGEMENT USED TO TEST AND MEASURE THE CHARACTERISTICS OF THE DEVELOPED SERVO DRIVE PROTOTYPE

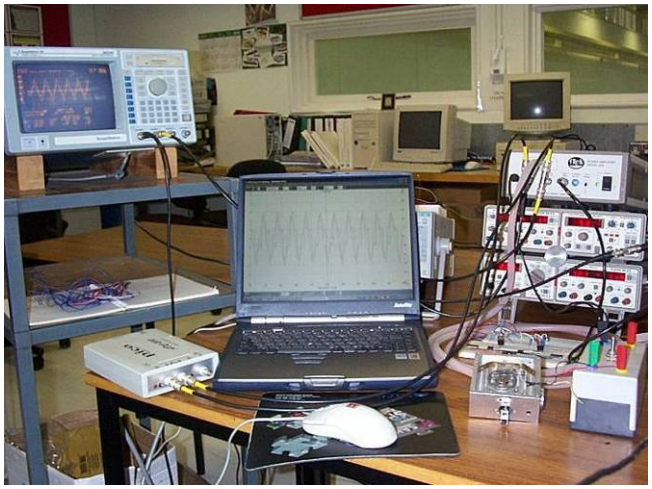

FIG. 10 ACTUAL TEST RIG ARRANGEMENT USED TO TEST AND MEASURE THE CHARACTERISTICS OF THE DEVELOPED USM PROTOTYPE

The speed of the USM was measured for each increment. It was noticed that during this process that the speed of the USM increased as the frequency of the driver increased. At one stage, the USM reached a maximum speed, and then started to decrease dramatically. Fig 12 shows the relationship between the travelling speed and frequency, indicating that the operating frequency for the developed prototype for no-load was 40.7 kHz. Figure 13 shows the travelling speed versus the input voltage. These measurements showed that the developed USM was able to provide a travelling speed of 28 mm/s, and a resolution on the order of micrometers.

The variation of the travelling speed versus the applied load was also measured at various loads, and shown in Fig. 14, indicating that the developed prototype was capable to carry a load up to 1.8 Newton which meets the requirements for electro discharge system industrial applications. The developed prototype had two directional of motion with un-similar characteristics as shown in Fig. 12, 13 and 14, as well as a wide range of frequency which enabled the control over the speed of the motor as illustrated in Figures 12 and 13. The varying frequency or the amplitude of the input signal controlled the traveling speed of the USM.

Design of the USM Electronic Driver

The design process of the developed USM piezoelectric driver passed through few steps. First, the technical operating parameters have been identified using off-shelf piezoelectric driver unit, see Fig. 10. This is allowed to define the USM operating frequency (40.7 KHz), voltage (50: 100 volt) and current (50: 100-mamp). Then the right design approach has been identified for the driver circuit.

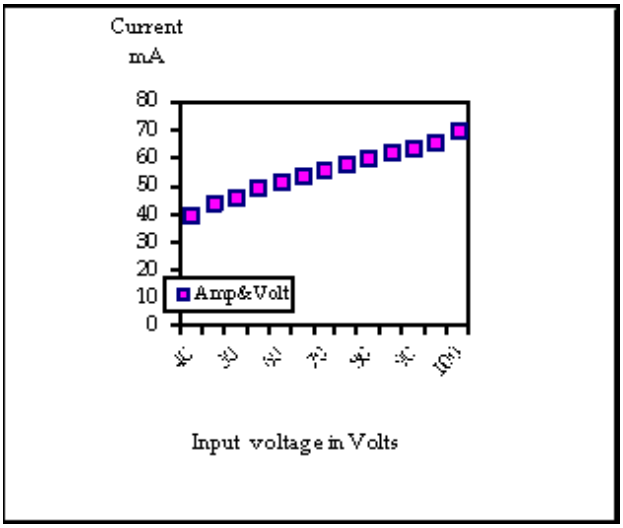

FIG. 11 THE VARIATION OF THE CURRENT VS. INPUT VOLTAGE FOR THE DEVELOPED USM PROTOTYPE (NO-LOAD APPLIED) [SHAFIK, M., 2003]

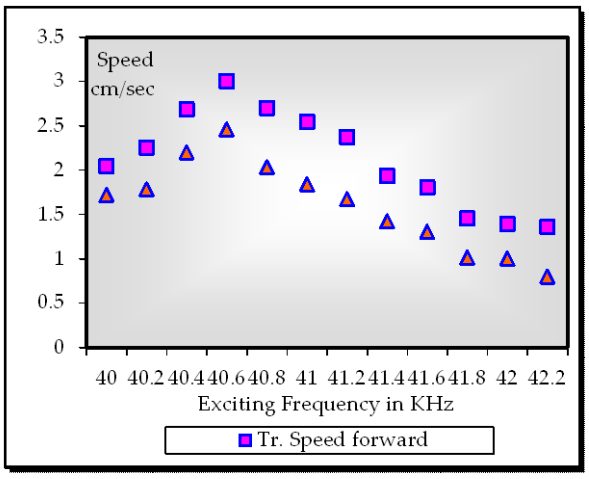

FIG. 12 THE VARIATION OF THE TRAVELLING SPEED VS. FREQUENCY FOR THE DEVELOPED USM PROTOTYPE (NO-LOAD APPLIED) [SHAFIK, M., 2003]

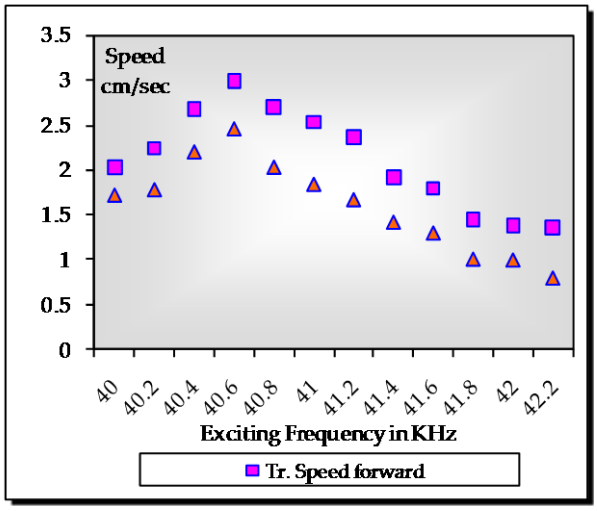

FIG. 13 THE VARIATION OF THE TRAVELLING SPEED VS. INPUT VOLTAGE FOR THE DEVELOPED USM PROTOTYPE (NO-LOAD APPLIED) [SHAFIK, M., 2003]

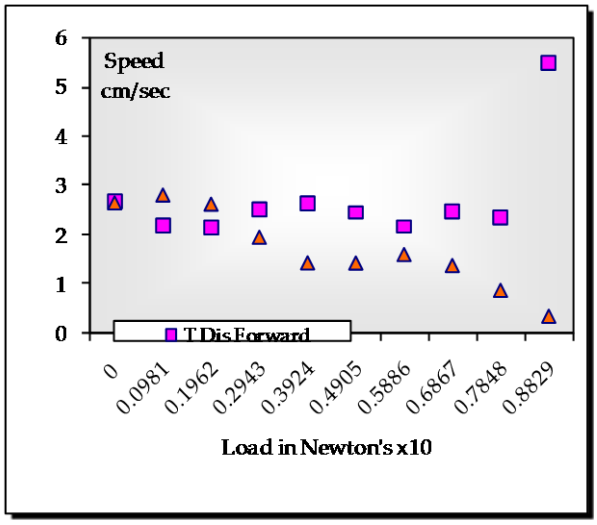

FIG. 14 THE VARIATION OF THE TRAVELLING SPEED VS. APPLIED LOAD FOR THE DEVELOPED USM PROTOTYPE [SHAFIK, M., 2003]

The approach is to use two stages, the first of which is a DC/DC converter that boosts 18 volt input to 80 volt, while the other is a piezo amplifier which consists of four output transistors, push-pull and bridge connected in order to achieve maximum amplitude.

The input signal to the amplifier is generated by an oscillator, op-amp circuitry. The output from the oscillator is low pass filtered in order to achieve a sine wave signal. The sine wave is then voltage amplified by a transistor to approx 50V before it is connected to the USM.

Installation of USM Servo Control Drive in EDM System

The developed Servo USM drive has been integrated, tested and validated in Electro Discharge Machining System. The developed system was evaluated compared to the exiting system using AC and DC servo feed drive. This included an investigation into the stability of the system, capability of control, processing time and surface finish of the textured products and was carried out using various electro-texturing parameters, including level of current, on/off time and duty cycle. Fig 15 shows the system installed in EDM A ELEKTRA R-50 ZNC model.

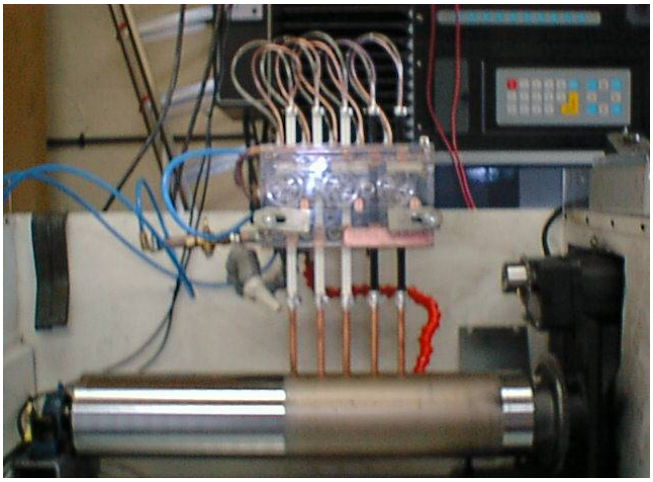

FIG. 15 THE DEVELOPED PIEZOELECTRIC USM SERVO FEED DRIVE INSTALLED IN THE EDT MACHINE (A ELEKTRA R-50 ZNC MODEL)

Experimental Test and Validation in EDM

The EDT-system is a variation of the EDM process. As with electro discharge die sinking, ED wiring, ED sawing and ED grinding, the major difference is in the configuration of the main elements of the machine. Here an experimental investigation into the current EDT-system and the developed control system using piezoelectric ultrasonic drive was conducted. The

current system, using DC servo feed drive, was used for texturing different areas using various electro-machining parameters. Then the developed system, using piezoelectric ultrasonic feed drive, was used for machining by means of the same electro-machining parameters and similar conditions. Texturing different sampled was carried out using the EDT machine. The levels of current, on-off time and duty cycle were used as main electro-machining parameters. The other machining parameters were selected as follows: The feed rate of the system in the case of auto position was 0.656 mm/sec, speed of the roll was 6 rpm, SEN = 1:3 [Sensitivity of Z-axis speed], ASEN = 3-9 [Antiarc sensitivity], TW =1.0 µsec [Sparking time], T = 0.5µsec [Lifetime], Vg = 38: 50 volts [Gap voltage], Ig = 5 amperes [Gap current], Ib = 0. 0 [Prepulse spark current], POL=-ve [Polarity of machining] and Fp=0.2 bar [Flushing pressure]. The feed rate in the case of the piezoelectric ultrasonic control system was of the order of 5.1 mm/sec. An evaluation for both control systems was also conducted. This included stability of the system, surface profiles (roughness, Pc peak/cm), capability of the system to monitoring and control of the inter-electrode gap, and safety of machining process.

The stability of the EDT and or EDM system can be distinguished from the inter electrode gap voltage and current in addition to the control signal obtained from the system control unit. Therefore, the feedback signal and inter-electrode gap voltage variation were obtained at various electro-machining parameters. Figures 16 and 17 illustrate the variations of these signals for various electro-machining parameters for both control systems. It showed the indication of the stability of machining for a period of 10 seconds. Fig 16 shows these variations for the existing control system using electric motor. Here it is notable that there is a clear instability on the feedback signal and the inter-electrode gap. Fig 17 shows the variation in the feedback control signal and inter-electrode gap voltage for the developed system. This shows the stability of machining, remarkable reduction in the arcing and short-circuiting processes, which in turn may lead to a clear reduction in the machining time when compared to the current system. It was also observed, during this investigation, that the increment in the required level of current had no major influence on the stability in the case of the piezoelectric USM system as in the case of the electric motor. Two factors showed an effect on the machining process, namely the sensitivity and the anti-arcing factor. The capability of changing the machining parameters during machining process was used in this case to select the optimum values, which provided a stable machining. It was noticed that mishandling the sensitivity and anti-arcing factors produced jerking effect led to unstable machining, which in turn increased the arcing and short-circuiting process and further causing poor surface profiles and increased the machining time of the process. This was clear in the case of the electric servomotor control system rather than the developed control system using piezoelectric USM.

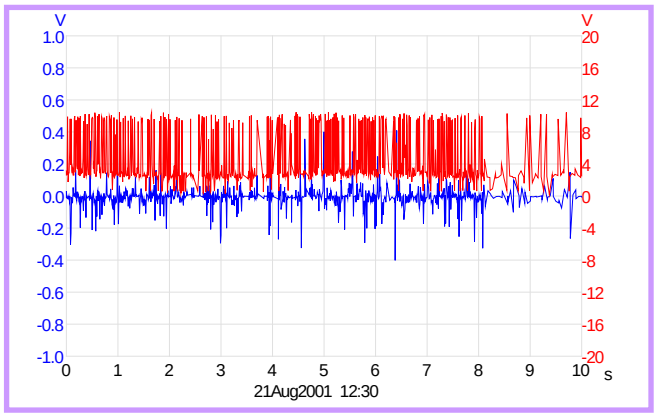

FIG. 16 FEEDBACK CONTROL SIGNAL AND INTER-ELECTRODE GAP VOLTAGE VARIATION FOR EDT MACHINING USING THE CURRENT DC SERVO CONTROL SYSTEM [GAP CURRENT 5A, GAP VOLTAGE OF 38 VOLTS & DUTY CYCLE 8µSEC] [SHAFIK, M., 2003]

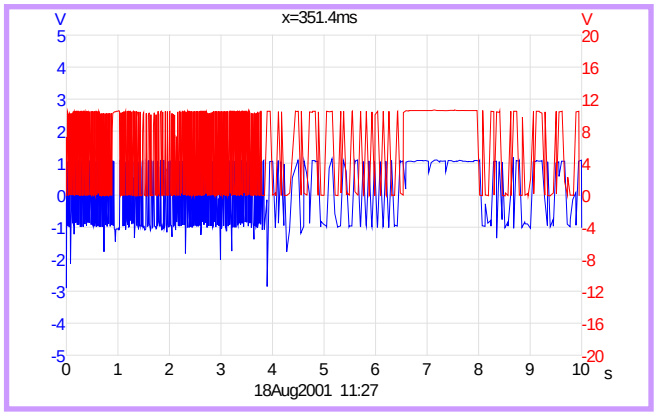

FIG. 17 FEEDBACK CONTROL SIGNAL AND INTER-ELECTRODE GAP VOLTAGE VARIATION FOR EDT MACHINING USING THE DEVELOPED PIEZOELECTRIC USM CONTROL SYSTEM [GAP CURRENT 5A, GAP VOLTAGE OF 38 VOLTS & DUTY CYCLE 8MSEC] [SHAFIK, M., 2003]

An electron microscopic investigation into the textured surface using EDT-system for both systems of control using current and developed system were carried out. Figures 18 and 19 show the scanning electron microscope image of the textured surface profiles using both control systems. These figures

show the investigations into the surface profiles machined using a different duty cycle. These show noticeably how the duty cycle was used to control the machined surface finish as well as the difference between the surface profiles obtained using piezoelectric USM system and electric servomotor system. It can be seen that there is a smooth surface obtained using the developed system as clarified in Fig 19. Figures 20 and 21 show a close investigation into the textured surface profiles for cross-section area 20 microns, evidently indicating the smooth surface finish obtained using piezoelectric USM control system compared with the EMM control system.

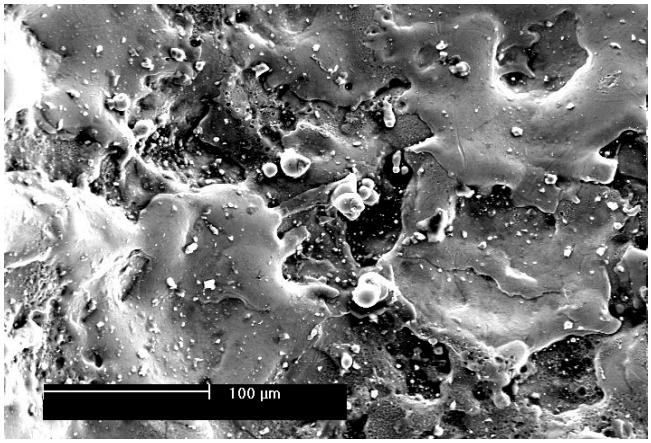

FIG. 18 EDM SURFACE FINISH OBTAINED USING DC SERVO CONTROL FEED SYSTEM USING CURRENT LEVEL OF 6 AMPERES, 'ON' TIME OF 50 µSEC, DUTY CYCLE OF 4 µSEC [SHAFIK, M., 2003]

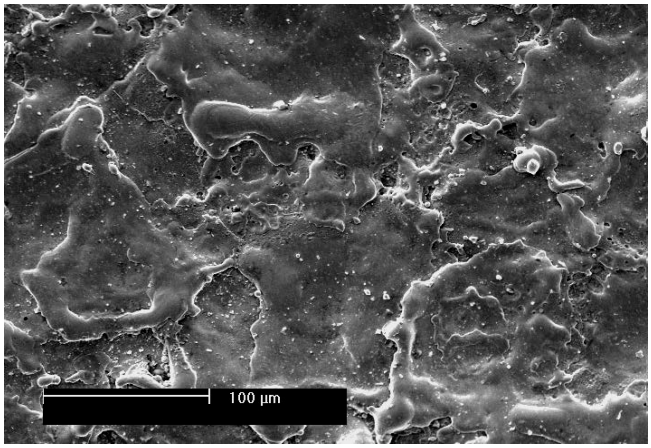

FIG. 19 EDM SURFACE FINISH OBTAINED USING USM SERVO CONTROL FEED SYSTEM USING CURRENT LEVEL OF 6 AMPERES, 'ON' TIME OF 50 µSEC, DUTY CYCLE OF 4 µSEC [SHAFIK, M., 2003]

A Taylor Hobson measuring system for surface finish was applied to measure the roughness and peak count of the various machined areas along the roll and carried out a few times for each sample and the average of the degree of texture was determined. The relationships between measured degree of roughness and peak count of the textured surfaces using both systems for control and various electro-machining parameters are shown in figures 22, 23, 24 and 25. Figures 22 and 23 show the variation of the degree of roughness, against peak-current, and on-off time, indicating a close agreement with the previous results obtained in this area of machining. It can be seen that the degree of roughness of the textured surface using both techniques of control was increased as the peak current and the on-off time increased. There was a small deviation in the degree of roughness of the bands machined using the developed system when compared to the existing electric servomotor system [McGeough, J. and Rasmussen, 1992, El-Menshawy, F., and Ahmed, M. S., 1985]. Figures 24 and 25 show the variation of the peak count against peak current and on-off time. Here it can be seen that the peak count decreased as the peak current and on-off time increased.

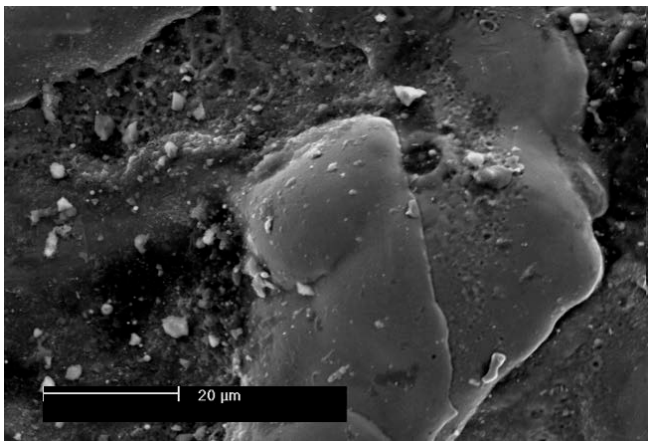

FIG. 20 EDT SURFACE PROFILES FROM THE DC CONTROL SYSTEM AND OPERATING PARAMETERS, CURRENT OF 6 AMPERES, 'ON' TIME OF 50 µSEC AND DUTY CYCLE OF 12 µSEC [SHAFIK, M., 2003]

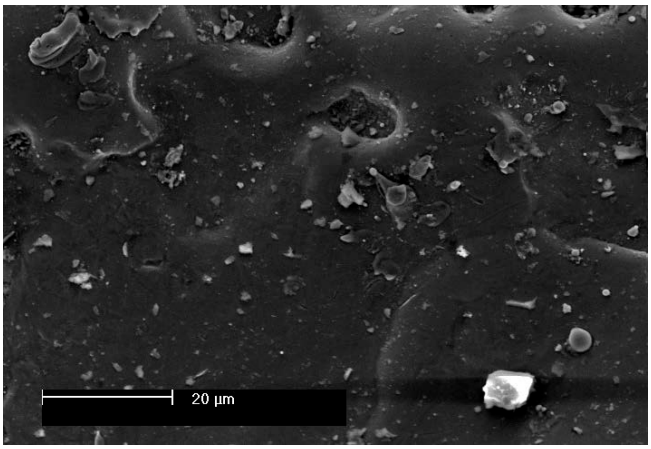

FIG. 21 EDT SURFACE PROFILES FROM THE USM CONTROL SYSTEM AND OPERATING PARAMETERS, CURRENT OF 6 AMPERES, 'ON' TIME OF 50 µSEC AND DUTY CYCLE OF 12 µSEC [SHAFIK, M., 2003]

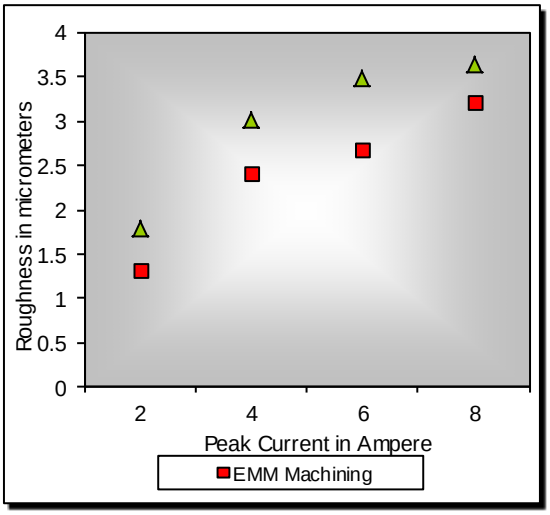

FIG. 22 THE DEGREE OF ROUGHNESS VERSUS THE MACHINING PARAMETERS FOR BOTH SYSTEMS OF CONTROL USING DC SERVOMOTOR AND USM [SHAFIK, M., 2003]

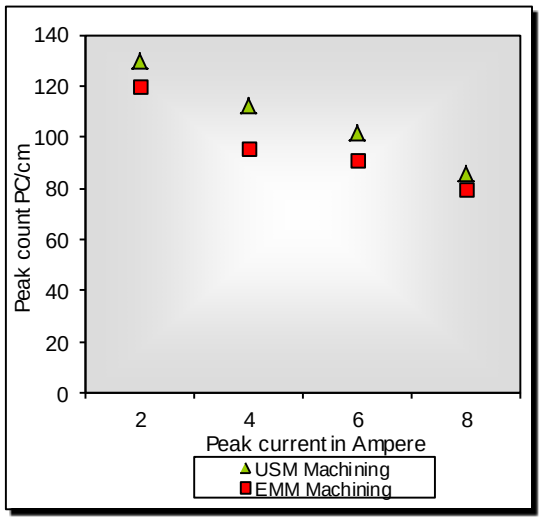

FIG. 23 VARIATION OF THE PEAK COUNT AGAINST VARIOUS PEAK CURRENT FOR BOTH SYSTEMS OF CONTROL USING DC AND USM MOTOR [SHAFIK, M., 2003]

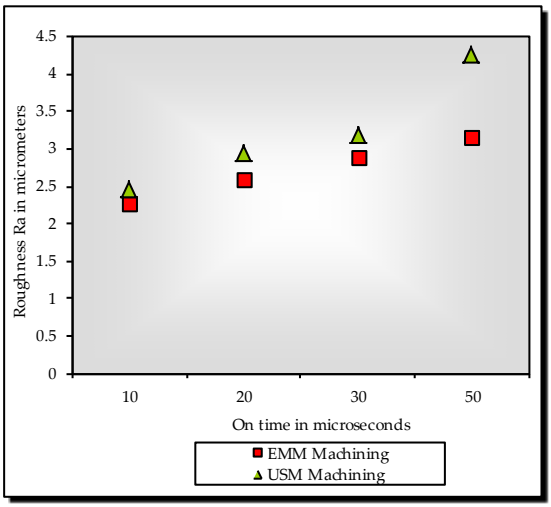

FIG. 24 VARIATION OF THE ROUGHNESS AGAINST ON TIME FOR BOTH SYSTEMS OF CONTROL USING DC AND USM MOTOR [SHAFIK, M., 2003]

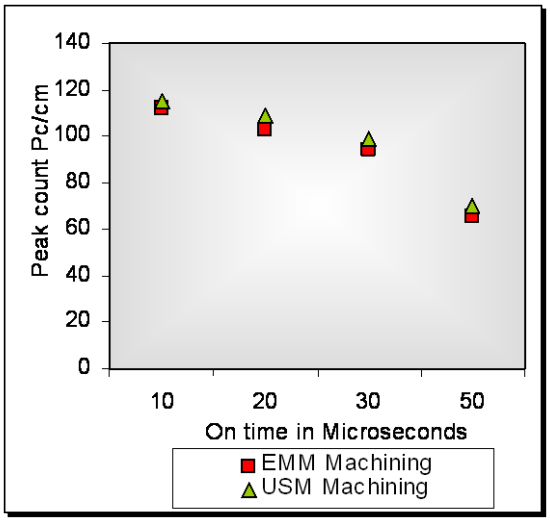

FIG. 25 VARIATION OF THE PEAK COUNT AGAINST ON/OFF TIME FOR BOTH SYSTEMS OF CONTROL USING DC AND USM MOTOR [SHAFIK, M., 2003]

Conclusions

A smart servo control feed drive for EDM/EDT material machining System industrial applications, using ultrasonic technology has been developed then tested and validated in EDT System application. Finite Element Analysis has been used in the ultrasonic servo drive design and development life cycle to examine and investigate the USM structure, material deformation, define the piezoelectric material specifications and determine the operating parameters of the USM. A prototype of the USM servo control feed drive was fabricated and the necessary practical tests to examine the USM drive reliability for EDM/EDT System industrial applications was also carried out. The results showed that the developed prototype operating parameters for no-load were frequency equal to 40.7 KHz, voltage: 50: 100 volt and current: 50: 100 m-amperes and that the drive was capable to provide a reversible directional of motion, no-load travelling speed equal to 28 mm per second, maximum load of 1.8 Newton, a resolution less than 50μm and a dynamic response in the order of microseconds. The developed servo control feed drive has been validated successfully in EDM/EDT applications. The initial results showed that a substantial improvement in the stability of machining was obtained when compared to the existing system using DC servomotor. This was verified by examining the electrode movements, the inter-electrode gap voltage, current and feedback control signals. The electron microscopic investigation into the surface profiles using both systems of control showed that

there was a visible improvement in the surface profiles processed by means of the USM servo control system. A notable reduction in the arcing and short circuit process was also observed. The relationship between the electro texturing parameters, and surface profiles roughness was obtained and presented, indicating a close agreement with the existing system with miner deviation in the degree of roughness.

ACKNOWLEDGEMENTS

The author would like particularly to thank, Professor J Knight and Professor R Bansevicius for their help, support and constructive discussion throughout this research. My deepest thanks also goes to Professor S Ahmed for his guidance and endless support.

REFERENCES

Aoyagi M., Tomikawa Y. and Takano T., Ultrasonic motors using longitudinal and bending multimode vibrators with mode coupling by external additional asymmetry or internal nonlinearty. *Japanese J. of Applied Physics part 1*, 31(9B), 3077-3080, 1992.

Aoyagi M. and Tomikawa Y., Ultrasonic motor based on coupled longitudinal-bending vibrators of a diagonally symmetry piezoceramic plate. *Electronics and Communications in Japan*, 79(6), 60-67, 1996.

Behrens, A., and Ginzel, J., "An open numerical control architecture for electro discharge machining", 13th international symposium for Electromachining, ISEM, Spain, May 9th to 11th, 2001.

Behrens, A., Ginzel, J. and Bruhns, F., "Arc detection in electro-discharge machining", 13th international symposium for Electromachining, ISEM, Spain, May 9th to 11th, 2001.

Chen, Y., Lu, K., Zhou, T.Y., Liu, T. and Lu, C.Y., Study of a mini-ultrasonic motor with square metal bar and piezoelectric plate hybrid. Jpn. J. Appl. Phys., 45(5B), 4780–4781, 2006.

Chiharu K, et al., Effect of the pressing force applied to a rotor on Disk type ultrasonic motor driven by self oscillation. *Japanese journal of applied Physics*, 37, 2966-2969, 1998.

El-Menshawy, F., and Ahmed, M. S., "Monitoring and control of the electrical discharge texturing process for steel cold mill work roll", *Proc. of 13th North American Research Conference*, 470-475, 1985.

Frangi, A., Corigliano, A., Binci, M. and Faure, P., Finite element modelling of a rotating piezoelectric ultrasonic motor. *Ultrasonics*, 43(9), 747–755, 2005.

Furutani, K. and Furuta, A. March, Evaluation of driving performance of piezoelectric actuator with current pulse. *10th IEEE International Workshop on Advanced Motion Control*, 26-28, 387 – 392, 2008.

Hosoe, "Ultrasonic motors for auto-focusing lenses" choonpa Techno, Vol. 1, No. 2, pp. 36-41., 1989.

Hwang W. S. and Park H. C., Finite element modelling piezoelectric sensors and actuators, *AIAA J*, 31(5), 930-937, 1993.

He S., Chen W., Tao X., and Chen Z., Standing wave bi-directional linearly moving ultrasonic motor. *IEEE Transactions on Ultrasonics, Ferroelectrics and Frequency Control*, 45(5), 1133-1139, 1998.

Izuno, Y., Izumi, T., Yasutsune, H., Hiraki, E. and Nakaoka, M., "Speed tracking servo control system incorporating travelling-wave-type ultrasonic motor and feasible evaluations", IEEE Transactions on Industry Applications, 34 (1): pp. 126-132, January-February, 1998.

Izuno, Y., and Nakaoka, M., "Ultrasonic motor actuated direct drive positioning servo control system using fuzzy reasoning controller", Electrical Eng. in Japan, Vol. 117, No. 6, pp. 74-84, 1996.

Ise, et al, "Three degree-of-freedom artificial forearm using ultrasonic motor", Keisoku Jido Seigyo Gakkai Ronbunshu, Vol. 27, No. 11, pp. 1281-1289, 1991.

Lin, F. J., Wai R. J. and Hong C. M., "Recurrent neural network control for LCC-resonant ultrasonic motor drive", IEEE Trans. on ultrasonics ferroelectrics and frequency control, 47 (3): 737-749, May, 2000.

Li, X., Chen, W.S., Tang, X. and Liu, J.K., Novel high torque bearingless two-sided rotary ultrasonic motor. Journal of Zhejiang University - Science A, 8(5), 786-792, 2007.

Lebrun, L., et al., A Low-cost piezoelectric motor using a (1,1) nonaxisymmetric Mode. *Smart Mater. Struct.* , 8(4), 469-475, 1999.

Lin M. W., Abatan A. O. and Rogers C. A., Application of commercial finite codes for the analysis of induced strain-Actuated structures. *Journal of Intelligent Material Systems and Structures*, 5(6), 869-875., 1994.

McGeough, J. and Rasmussen, H., "A model for the surface texturing of steel rolls by electro discharge machining", *Proceedings: Mathematical and Physical Sciences,* 436, 155-164, 1992.

Ming, Y. and Que, P. W., Performance estimation of a rotary traveling wave ultrasonic motor based on two-dimension analytical model. *Ultrasonics,* 39(2) 115-120, 2001.

Shafik, M., 'Computer Aided Analysis and Design of a New Servo Control Feed Drive for EDM using Piezoelectric USM', PhD Thesis, De Montfort University, Leicester, UK, 2003.

Shafik M. & H. S. Abdalla, 'A Micro Investigation into Electro Discharge Machining Industrial Applications Processing Parameters and Surface Profile Using a Piezoelectric Ultrasonic Feed Drive', ASME, J. Manuf. Sci. Eng. August 2011, Volume 133, Issue 4, 044503 (7 pages) DOI: 10.1115/ 1.4004687, USA, 2011.

Shafik M., Knight J. and Abdalla H. 2001. "Development of a new generation of electrical discharge texturing system using an ultrasonic motor", *13th International Symposium for Electromachining*, Spain , *ISEM*, 9 -11 May 2001.

Shafik M., et al, "Computer Simulation and Modelling of Standing Wave Piezoelectric Ultrasonic Motor Using Flexural Transducer, ASME 2012 International Mechanical Engineering Congress and Exposition, Houston, TX, USA, 2012.

Shafik M., et al, "An Investigation into the Influence of Ultrasonic Servo Drive Technology in Electro Discharge Machining Industrial Applications", ASME 2012 International Mechanical Engineering Congress and Exposition, Houston, TX, USA, 2012.

Simao J, Aspinwall D, El-Menshawy F and Ken Meadows K., "Surface alloying using PM composite electrode materials when electrical discharge texturing hardened AISI D2", *Journal of Materials Processing Technology*, 127 (2), 211-216, 2002.

Shafik M., Knight J., Computer simulation and modelling of an ultrasonic motor using a single flexural vibrating bar. *Proceeding of ESM'2002 International Conference*, 3 – 5 June, Germany, 2002.

Snitka V., Ultrasonic actuators for nanometer positioning. *Ultrasonics*, 38 (1-8), 20-25, 2000.

Newton D., Garcia E. and Horner G. C., A Linear piezoelectric motor. *Smart Materials and Structures*, 6, 295-304, 1997.

Takano T., Tomikawa Y. and Takano C.K., Operating characteristics of a same-phase drive-type ultrasonic motor using a flexural disk vibrator. *Japanes J. of Applied physics part 1*- 1999, 38(5B), 3322-3326, 1999.

Tal, J. 1999, Servomotors take piezoceramic transducers for a ride. *Machine Design,* 71(23), 1-3.

Tobias H. and Wallaschek J., Survey of the present state of the art of piezoelectric linear motors. *Ultrasonics*, 38, 37-40, 2000. www.nanomotion.net

Zhang B. and Zhenqi Z., Developing a linear piezomotor with nanometer resolution and high stiffness. *IEEE/ASME Transaction on Mechatron*, 2(1), 22-29, 1997.

Zhang, F., Chen, W., Lin, J. and Wang, Z., Bidirectional linear ultrasonic motor using longitudinal vibrating transducers. *IEEE Transactions on Ultrasonics, Ferroelectrics and Frequency Control,* 52(1), 134-138, 2005.

Biographical Notes

Dr. Mahmoud Shafik is a Reader in Mechatronics Engineering and Principal Technology Investigator at School of Technology, Faculty of Art & Design and Technology, University of Derby, UK. He received his BEng honour degree in engineering from Cairo, Egypt, 1993. After graduation, he joined the Department of Aerospace for three years as a chartered Engineer. In 1996, he moved to the Cairo International Research Centre, during this time he received his master degree in Autonomous Control System, from the same university of graduation. In 1st of October 98, he was offered a Ph.D. studentship at De Montfort University, Leicester, UK, and at the end of 2000 he received his MPhil in Mechatronics and in the beginning of 2003 he has been awarded his PhD in Mechatronics Engineering. In 2001 he was offered a post doctor research fellow at De Montfort University, UK, in 2004 he moved to the University of Cyprus, as an Associate Professor, during this time he was the technical innovation consultant of Nexsis Technology Group. In 2005 Dr Shafik joined Pera Innovation Group, UK as a Principal Technology Investigator. For more information of Dr Shafik profile, projects and achievements please visit: http://uk.linkedin.compub/mahmoud-shafik/7/237/60, http://diamond.pera.com/,http://pyrotect.pera.com/,http://humid.pera.com/.http://radical.pera.com/,http://actuator.pera.com/..